

COSMIC TRAIN WRECK BY MASSIVE BLACK HOLES: DISCOVERY OF A KPC-SCALE TRIPLE ACTIVE GALACTIC NUCLEUS¹

XIN LIU^{2,3}, YUE SHEN², AND MICHAEL A. STRAUSS⁴

Received 2011 April 17; accepted 2011 June 10; to appear in ApJL

ABSTRACT

Hierarchical galaxy mergers will lead to the formation of binary and, in the case of a subsequent merger before a binary coalesce, triple supermassive black holes (SMBHs), given that most massive galaxies harbor SMBHs. A triple of SMBHs becomes visible as a triple active galactic nucleus (AGN) when the BHs accrete large amounts of gas at the same time. Here we report the discovery of a kpc-scale triple AGN, SDSS J1027+1749 at $z = 0.066$, from our systematic search for hierarchical mergers of AGNs. The galaxy contains three emission-line nuclei, two of which are offset by 450 and 110 km s⁻¹ in velocity and by 2.4 and 3.0 kpc in projected separation from the central nucleus. All three nuclei are classified as obscured AGNs based on optical diagnostic emission line ratios, with black hole mass estimates $M_{\bullet} \gtrsim 10^8 M_{\odot}$ from stellar velocity dispersions measured in the associated stellar components. Based on dynamical friction timescale estimates, the three stellar components in SDSS J1027+1749 will merge in ~ 40 Myr, and their associated SMBHs may evolve into a gravitationally interacting triple system in $\lesssim 200$ Myr. Our result sets a lower limit of $\sim 5 \times 10^{-5}$ for the fraction of kpc-scale triples in optically selected AGNs at $z \sim 0.1$.

Subject headings: black hole physics — galaxies: active — galaxies: interactions — galaxies: nuclei — galaxies: stellar content

1. INTRODUCTION

Galaxies are thought to be built up hierarchically via mergers (Toomre & Toomre 1972). Because most massive galaxies are believed to harbor a central supermassive black hole (SMBH; Kormendy & Richstone 1995), galaxy mergers will result in the formation of binary SMBHs through dynamical friction (Begelman et al. 1980; Milosavljević & Merritt 2001; Yu 2002). When a binary does not coalesce before a subsequent merger with a third galaxy, a system of three gravitationally interacting SMBHs is expected to form (e.g., Valtonen 1996). Triple SMBHs may hold important clues to our general understanding of massive galaxy formation. For example, numerical simulations suggest that triple SMBHs scour out cores in stellar bulges with mass deficits one or two times of the total mass of the BHs and sizes larger than those formed around binary SMBHs. This process may be responsible for the large cores observed in some massive elliptical galaxies such as M87 (Hoffman & Loeb 2007). Triple SMBHs also provide a unique astrophysical laboratory to study the chaotic dynamics of three-body interactions in General Relativity (e.g., Blaes et al. 2002; Merritt 2006). Numerical simulations of the dynamics of triples suggest that their encounter may lead to a merger of all three BHs, formation of a highly eccentric binary, or ejection of three free BHs (Iwasawa et al. 2006; Lousto & Zlochower 2008). Triple SMBHs exhibit phases of very high eccentricity in the inner binary, producing intense bursts of gravitational radiation which will be within the sensitivity range of forthcoming pulsar timing arrays and the Laser Interferometer Space Antenna (e.g., Amaro-Seoane et al. 2010).

Despite their significant scientific merit and intense theoret-

ical interest, direct observational evidence for gravitationally interacting triple SMBHs is still lacking, however, because their typical separation (less than a few parsecs) is too small to be resolved at cosmological distances. In this Letter, we report the probable discovery of a kpc-scale triple of SMBHs, at a separation large enough that the components can be easily resolved using current facilities, yet small enough for the system to be dynamically interesting. Using a simple stellar dynamical friction argument, we estimate that the system will form a bound SMBH triple in $\lesssim 200$ Myr. A triple of SMBHs becomes visible as a triple active galactic nucleus (AGN) when the BHs accrete large amounts of gas at the same time – a process which is thought to be common in gas-rich mergers (e.g., Hernquist 1989). While kpc-scale triple AGNs are supposed to be present in recurrent galaxy mergers, only one candidate is known⁵. It is a triplet of emission-line nuclei (with two offset nuclei at 5.1 and 8.4 kpc in projection from the primary nucleus) in the minor merger NGC 3341 at $z \sim 0.03$ serendipitously discovered by Barth et al. (2008).

To quantify the frequency of kpc-scale binary and triple systems of SMBHs, we are conducting a systematic search for hierarchical mergers of AGNs in the Seventh Data Release (DR7; Abazajian et al. 2009) of the Sloan Digital Sky Survey (SDSS; York et al. 2000). We have selected a sample of 1286 AGN pairs with projected separations $r_p < 100$ kpc and line-of-sight velocity offsets $\Delta v < 600$ km s⁻¹ (Liu et al. 2011b). Ninety-two AGN pairs in the sample have $r_p < 10$ kpc and $z < 0.16$. Seven of these 92 pairs have a third galaxy or nuclei with $r_p < 10$ kpc from both of the first two nuclei and r -band magnitude differences < 4 mag. Because of its proximity with the first two nuclei, none of the third nuclei has an SDSS spectrum due to the finite size of SDSS fibers⁶. To determine

¹ This paper includes data gathered with the Apache Point Observatory 3.5-meter telescope, which is owned and operated by the Astrophysical Research Consortium.

² Harvard-Smithsonian Center for Astrophysics, 60 Garden St., Cambridge, MA 02138

³ Einstein Fellow

⁴ Princeton University Observatory, Princeton, NJ 08544

⁵ There is one probable physical triple quasar known, QQ 1429–008 at $z \sim 2.1$ (Djorgovski et al. 2007), but the projected separations between the quasar components are much larger, ~ 30 –50 kpc.

⁶ The first two nuclei both have an SDSS spectrum because they were observed on overlapping spectroscopic plates.

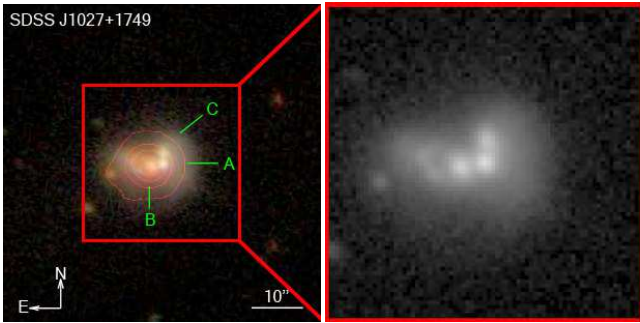


FIG. 1.— *Left*: SDSS *gri*-color composite image of SDSS J1027+1749, shown with a $1' \times 1'$ FOV. Contours indicate radio flux densities from the FIRST 1.4 GHz survey (Becker et al. 1995). The galaxy has three nuclei A, B, and C, and a strong tidal feature to the northeast of B. Nucleus B (C) has a projected separation of 3.0 (2.4) kpc from A. *Right*: SDSS *r*-band image of the central $30'' \times 30''$ region.

whether the third nucleus is also active and physically close to the first two nuclei, we are conducting spatially resolved spectroscopy for these kpc-scale triple AGN (hereafter, triple AGN, for short) candidates. Here, we report our initial results on the discovery of a triple AGN in a hierarchical merging system, SDSS J1027+1749. Shown in Figure 1, the galaxy contains three nuclei as seen in its SDSS image, with B and C at projected separations of 3.0 and 2.4 kpc from A. The nuclei A and B have SDSS spectra. We have conducted optical slit spectroscopy for all three nuclei. We describe our observations and data analysis in §2, and present physical measurements of the three nuclei in §3. We discuss implications of our results and conclude in §4. A Λ CDM cosmology with $\Omega_m = 0.3$, $\Omega_\Lambda = 0.7$, and $h = 0.7$ is assumed throughout.

2. OBSERVATIONS AND DATA ANALYSIS

We obtained slit spectra for SDSS J1027+1749 on the nights of 2011 March 2 and 6 UT using the Dual Imaging Spectrograph (DIS) on the Apache Point Observatory 3.5 m telescope. The sky was mostly non-photometric, with seeing ranging between $0.''8$ and $2.''0$ with a median around $1.''2$. DIS has a $4' \times 6'$ FOV with a pixel size of $0.''414$. We adopted a $1.''5 \times 6'$ slit with the B1200+R1200 gratings centered at 510 and 700 nm. The spectral coverage was 450–560 (640–760) nm with an instrumental resolution of $\sigma_{\text{inst}} \approx 60$ (30) km s^{-1} and a dispersion of 0.62 (0.58) \AA pixel^{-1} in the blue (red). We oriented the slit with PA = 105° , 133° , and 172° to go through the nuclei A and B, B and C, and A and C respectively, as labeled on the SDSS image shown in Figure 1. The total effective exposure time was 10800, 8100, and 8100 s for A, B, and C, respectively. Standard stars G191B2B and HZ44 were observed for spectrophotometric calibration. We reduced the DIS data following standard IRAF⁷ procedures (Tody 1986). We extracted one-dimensional spectra using $3''$ diameter apertures for the nuclei A, B, and C respectively. We applied a telluric correction from standard stars on the extracted one-dimensional spectra. The median signal-to-noise ratio (S/N) achieved was 50–80 pixel^{-1} .

Figure 2 shows the resulting rest-frame one-dimensional spectra and our best-fit models for the stellar continuum and the continuum-subtracted emission lines, respectively. We measure redshift by fitting the continuum with galaxy templates produced by population synthesis models

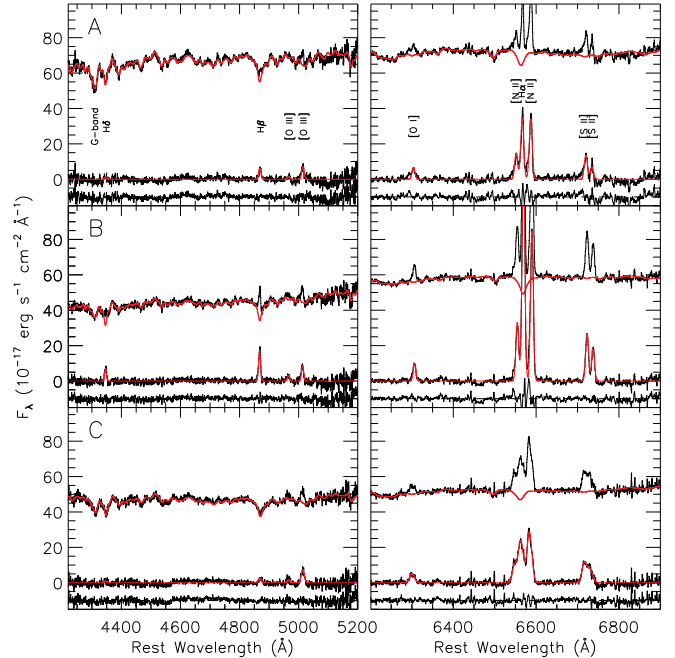


FIG. 2.— DIS one-dimensional spectra of the three nuclei of SDSS J1027+1749. We show the total spectra, the continuum-subtracted emission lines, and the continuum-and-emission-subtracted residuals offset by -10^{-16} $\text{erg s}^{-1} \text{cm}^{-2} \text{\AA}^{-1}$. Plotted in red are our best-fit models for the continuum and emission lines, respectively.

of Bruzual & Charlot (2003) using the procedure described in detail in Liu et al. (2009). The templates have been convolved with the stellar velocity dispersions σ_* measured over the spectral region of 4130–4600 \AA containing the G band $\lambda 4304 \text{\AA}$ using the direct fitting algorithm of Greene & Ho (2006) and Ho et al. (2009) following the procedure described in Liu et al. (2009). After subtracting the stellar continuum, we fit the emission lines simultaneously with Gaussian models constrained to have the same redshift and width.

3. RESULTS

Tables 1 and 2 list our measurements of the host and emission-line properties of the three nuclei of SDSS J1027+1749, respectively. The redshifts measured from stellar continuum fitting show that the components B and C are offset from A by ~ 450 and ~ 110 km s^{-1} in velocity. Their stellar velocity dispersions σ_* are 200–300 km s^{-1} , typical of massive galaxies at $z \sim 0.1$ of similar luminosities and sizes (Bernardi et al. 2003). To securely separate the three components, we applied aperture photometry for them individually with $3''$ diameter (corresponding to 3.8 kpc) apertures using their SDSS images. They all fall in the red sequence on the $u-r$, M_r color–magnitude diagram (Baldry et al. 2004). We have also performed surface brightness profile fitting using the GALFIT package (Peng et al. 2010), using stars within the field to model the point-spread function (PSF). Assuming a five-component model for the entire galaxy (four Sérsic profiles for the three nuclei and the surrounding diffuse component, and an exponential disk for the tidal feature), we estimate their *r*-band Sérsic indices as 1.4, 4.1, and 1.2 for A, B, and C, respectively. While the fit seems reasonable with a reduced χ^2 of 1.2, the results are highly uncertain given the limited resolution (*r*-band PSF FWHM $\sim 1.''1$) of the SDSS images and systematic uncertainties from model degeneracy. *Hubble Space Telescope* (HST) and/or ground-based imaging assisted with adaptive optics will help better determine their

⁷ IRAF is distributed by the National Optical Astronomy Observatory, which is operated by the Association of Universities for Research in Astronomy, Inc., under cooperative agreement with the National Science Foundation.

TABLE 1
HOST-GALAXY MEASUREMENTS OF THE THREE NUCLEI OF SDSS J1027+1749.

ID (1)	SDSS Designation (2)	z (3)	r (mag) (4)	M_r (mag) (5)	$M_{r,c}$ (mag) (6)	$u-r$ (mag) (7)	R_e (kpc) (8)	$\log M_*$ (M_\odot) (9)	$\log M_{*,c}$ (M_\odot) (10)	σ_* (km s $^{-1}$) (11)	$\log M_\bullet$ (M_\odot) (12)
A.....	J102700.40+174900.8	0.0668	16.73	-20.66	-22.4	2.48	1.1	10.4	11.2	265 ± 6	8.6
B.....	J102700.55+174900.2	0.0664	17.00	-20.38	-23.1	2.46	1.6	10.1	11.2	193 ± 10	8.1
C.....	J102700.38+174902.6	0.0652	17.03	-20.30	-24.5	2.51	2.4	10.2	12.0	305 ± 12	8.9

NOTE. — Col. 1: ID of the three nuclei as labeled on Figure 1; Col. 2: SDSS names with J2000 coordinates given in the form of “hhmmss.ss+ddmmss.s”; Col. 3: redshift measured from stellar continuum fitting; Col. 4: SDSS r -band fiber magnitude; Col. 5: SDSS r -band fiber absolute magnitude; Col. 6: Col. 5 after correction for internal dust extinction estimated using the Balmer decrement method; Col. 7: SDSS color from fiber magnitudes; Col. 8: effective radius from aperture photometry; Col. 9: stellar mass estimates from population synthesis modeling of the optical stellar continuum; Col. 10: Col. 9 after correction for internal dust extinction; Col. 11: stellar velocity dispersion from model fits of the stellar continuum over the G-band $\lambda 4304 \text{ \AA}$ region (Figure 2). The quoted errors throughout this table are statistical uncertainties; Col. 12: black hole mass estimates assuming the M_\bullet - σ_* relation of Tremaine et al. (2002) observed in local inactive galaxies.

TABLE 2
EMISSION-LINE MEASUREMENTS OF THE THREE NUCLEI OF SDSS J1027+1749.

ID (1)	$\log L_{[\text{O III}]}$ (L_\odot) (2)	$\log L_{[\text{O III}],c}$ (L_\odot) (3)	σ_{gas} (km s $^{-1}$) (4)	$[\text{O III}]/\text{H}\beta$ (5)	$[\text{N II}]/\text{H}\alpha$ (6)	$[\text{O I}]/\text{H}\alpha$ (7)	$[\text{S II}]/\text{H}\alpha$ (8)	$\text{H}\alpha/\text{H}\beta$ (9)	$\text{EW}_{\text{H}\alpha}$ (\AA) (10)	$\log n_e$ (cm $^{-3}$) (11)	$E(B-V)$ (mag) (12)
A.....	6.35	7.2	248 ± 17	1.2 ± 0.1	0.98 ± 0.02	0.18 ± 0.01	0.61 ± 0.02	5.3 ± 0.4	4.5 ± 0.1	-2.0	0.61 $^{+0.06}_{-0.09}$
B.....	6.38	7.7	211 ± 6	0.52 ± 0.03	0.66 ± 0.01	0.074 ± 0.003	0.35 ± 0.01	7.2 ± 0.2	19.1 ± 0.1	0.3 $^{+1.3}_{-2.3}$	0.93 $^{+0.02}_{-0.03}$
C.....	6.42	8.4	301 ± 23	3.2 ± 0.6	1.22 ± 0.01	0.21 ± 0.01	0.81 ± 0.02	12.1 ± 2.0	6.8 ± 0.1	1.9 $^{+0.2}_{-0.7}$	1.5 $^{+0.1}_{-0.3}$

NOTE. — Col. 1: same as Col. 1 in Table 1; Col. 2: $[\text{O III}] \lambda 5007$ luminosity from Gaussian fits to the emission lines; Col. 3: Col. 2 after correction for internal dust extinction estimated using the Balmer decrement method as listed in Col. 12; Col. 4: gas velocity dispersion from Gaussian fits of the continuum-subtracted emission lines (Figure 2). The quoted 1σ errors throughout this table are statistical uncertainties; Cols. 5–9: intensity ratios from Gaussian fits of the emission lines; Col. 10: rest-frame $\text{H}\alpha$ equivalent width; Col. 11: electron density estimated using the emission-line intensity ratio $[\text{S II}] \lambda 6717/[\text{S II}] \lambda 6731$. Col. 12: color excess estimated from the emission-line intensity ratio $\text{H}\alpha/\text{H}\beta$ (Col. 9) using the Balmer decrement method, assuming the intrinsic case B values of 2.87 for $T = 10^4 \text{ K}$ (Osterbrock 1989) and the extinction curve of Cardelli et al. (1989) with $R_V = 3.1$.

structural properties. We estimate stellar mass M_* based on population synthesis modeling of the optical stellar continuum. The stellar mass ratio of the triple system A : B : C is 2 : 1 : 1.3 before extinction correction and is 1 : 1 : 6 after. We estimate internal dust extinction from the emission-line intensity ratio $\text{H}\alpha/\text{H}\beta$ using the Balmer decrement method (Osterbrock 1989) assuming the intrinsic case B values of 2.87 for $T = 10^4 \text{ K}$ (Osterbrock 1989) and the extinction curve of Cardelli et al. (1989) with $R_V = 3.1$. However, the estimates are highly uncertain due to the systematic uncertainty in the dust geometry. The three stellar components are blended in Two Micron All Sky Survey (2MASS; Skrutskie et al. 2006). Higher resolution IR imaging is needed to better constrain their individual stellar masses.

Figure 2 shows that all the three nuclei emit narrow lines with gas velocity dispersions of $\sigma_{\text{gas}} \sim 200\text{--}300 \text{ km s}^{-1}$ (Table 2), consistent with σ_* of their associated stellar components. Their emission line intensity ratios (Table 2) are all characteristics of AGNs or AGN-H II composites. The masses of the AGNs are estimated to be $M_\bullet \gtrsim 10^8 M_\odot$ (Table 1) from σ_* of their associated stellar components⁸. Figure 3 shows the BPT diagram (Baldwin et al. 1981; Veilleux & Osterbrock 1987) for the three nuclei. Based on $[\text{N II}] \lambda 6584/\text{H}\alpha$ and $[\text{O III}] \lambda 5007/\text{H}\beta$, A is classified as a low-ionization narrow emission region (LINER), B is a composite, and C is a Seyfert (or a LINER within uncertainties). A (C) is consistently classified as a LINER (Seyfert) based on diag-

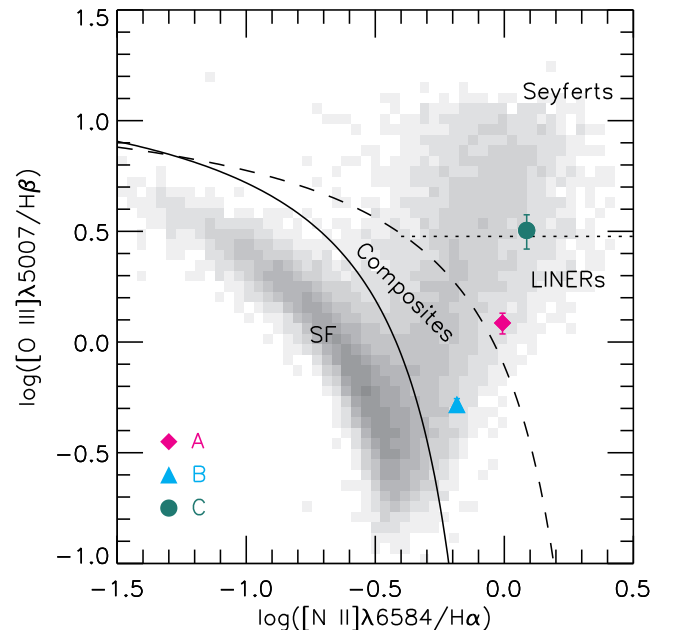


FIG. 3.— Optical diagnostic emission-line ratios for the three nuclei measured from the continuum-subtracted slit spectra (Figure 2). Gray scales indicate number densities of 31,179 emission-line galaxies from the SDSS DR4 (Kauffmann et al. 2003). The solid curve is the empirical separation between H II regions and AGNs (Kauffmann et al. 2003), and the dashed curve is the theoretical “starburst limit” (Kewley et al. 2006). Pure star-forming (SF) galaxies lie below the solid curve, AGN-dominated galaxies lie above the dashed curve, and AGN-H II composites lie in between. The dotted curve is the empirical separation between Seyferts and LINERs (Ho et al. 1997).

⁸ This still holds after correcting for the fact that M_\bullet is likely overestimated by ~ 0.2 dex using σ_* measured in AGN mergers separated by a few kpc (Liu et al. 2011a).

nostic ratios $[\text{S II}] \lambda\lambda 6717, 6731/\text{H}\alpha$ or $[\text{O I}] \lambda 6300/\text{H}\alpha$ and $[\text{O III}] \lambda 5007/\text{H}\beta$ according to the criteria of Kewley et al. (2006). While LINERs and composites may be due to stellar or shock heating rather than AGN excitation (e.g., Lutz et al. 1999), X-ray observations show that $\sim 80\%$ of them do harbor AGNs (e.g., Ho 2008). Because the intrinsic AGN luminosities of the three nuclei are obscured in the optical, we estimate the intrinsic hard X-ray luminosity $L_{X,2-10\text{keV}}$ using the $[\text{O III}] \lambda 5007$ luminosity (corrected for internal extinction; Table 2) as a surrogate⁹, finding $\log(L_{X,2-10\text{keV}}/\text{erg s}^{-1}) \approx 42.4, 43.0, \text{ and } 43.9$ for A, B, and C, respectively. The non-detection of the system in the *ROSAT* All-Sky Survey (Voges et al. 1999) is consistent with these estimates. The intrinsic $[\text{O III}] \lambda 5007$ luminosities and $\text{H}\alpha$ equivalent widths (Table 2) are typical of $z \sim 0.1$ obscured AGNs (e.g., Kauffmann et al. 2003; Ho 2008). The component B has a strong post-starburst component, as indicated by the strong Balmer absorption in our slit spectrum. This is also seen in its SDSS fiber spectrum which covers the higher order Balmer series and the Balmer break. B is also detected in the FIRST 1.4 GHz survey with an integrated flux density of 13.57 ± 0.14 mJy (Becker et al. 1995). The galaxy is contained in the *IRAS* faint source catalog (Moshir et al. 1992) with a positional match centered on B, IRAS 10242+1804, with an IR (1–1000 μm) luminosity of $L_{\text{IR}} \sim 10^{11.3} L_{\odot}$ estimated based on its flux densities at 60 and 100 μm from *IRAS* using the formulae of Helou et al. (1988).

4. DISCUSSION

Based on dynamical friction timescale estimates¹⁰, the stellar components B and C will merge with A in $t_{\text{fric}} \sim 40$ and ~ 8 Myr, respectively, corrected for projection assuming random orientation for r_p . The three SMBHs will inspiral with their individual stellar bulges at first, but will then decay to the center of the merged galaxy under dynamical friction with the stellar background in $\sim 40\text{--}200$ Myr¹¹, given their mass estimates (Table 1). However, the actual evolution involving three comparable stellar components and the associated gas is likely more complicated. High resolution kinematics observations (e.g., Amram et al. 2007) combined with tailored numerical modeling (e.g., Renaud et al. 2010) are needed to unravel the merger history and future of this triple system. Regardless of the actual sequence of the mergers, the SMBHs may form a gravitationally interacting triple system, if the orbit of the third SMBH decays rapidly before the first two

⁹ Measurements of $L_{X,2-10\text{keV}}/L_{[\text{O III}]}$ for optically selected obscured AGNs range from a few to a few hundred (e.g., Heckman et al. 2005; Panessa et al. 2006). Here, we adopt the mean calibration of Panessa et al. (2006), $\log(L_{X,2-10\text{keV}}/\text{erg s}^{-1}) = 1.22 \log(L_{[\text{O III}]}/\text{erg s}^{-1}) - 7.34$.

¹⁰ Assuming singular isothermal spheres for the density profiles and circular orbits, the dynamical friction timescale for a satellite galaxy with velocity dispersion σ_S inspiraling from radius r in a host galaxy with velocity dispersion σ_H can be estimated as $t_{\text{fric}} = \frac{2.7}{\ln \Lambda} \frac{r}{30 \text{ kpc}} \left(\frac{\sigma_H}{200 \text{ km s}^{-1}} \right)^2 \left(\frac{100 \text{ km s}^{-1}}{\sigma_S} \right)^3$ Gyr, where Λ is the Coulomb logarithm (Binney & Tremaine 1987). $\ln \Lambda \sim 2$ for equal mass mergers (Dubinski et al. 1999). We assume A as the host, and B and C as satellites, since A is at the apparent center of the galaxy. Assuming C as the host instead, which has the largest σ_* , yields similar estimates for t_{fric} , ~ 20 Myr for A and C, and ~ 70 Myr for B and C, respectively.

¹¹ Assuming a singular isothermal sphere for the density distribution of the host galaxy, the dynamical friction timescale of a BH of mass M_{\bullet} on a circular orbit of radius r can be estimated as $t_{\text{fric}} = \frac{19}{\ln \Lambda} \left(\frac{r}{5 \text{ kpc}} \right)^2 \frac{\sigma_H}{200 \text{ km s}^{-1}} \frac{10^8 M_{\odot}}{M_{\bullet}}$ Gyr, where $\ln \Lambda \sim 6$ for typical values (Binney & Tremaine 1987). We estimate that $t_{\text{fric}} \sim 200$ and 40 Myr for the SMBHs in B and C, to reach the center of the merger products of B and C with A, respectively.

SMBHs merge.

The fraction of kpc-scale pairs of AGNs is $f_{\text{kpc, double}} \gtrsim 3 \times 10^{-3}$ corrected for SDSS spectroscopic incompleteness based on the number of AGN pairs with $r_p < 10$ kpc found in our parent AGN sample (Liu et al. 2011b; see also Liu et al. 2010 and Shen et al. 2011 for a similar estimate of $f_{\text{kpc, double}}$ from a complementary approach to identify kpc-scale AGN pairs, based on the selection of AGNs with double-peaked narrow emission lines). This is a lower limit due to the limited imaging resolution of SDSS. Out of the seven kpc-scale triple AGN candidates, we have obtained slit spectra for five systems, including SDSS J1027+1749. The nature of the other four systems seems less clear, due to alternative scenarios involving star clusters or tidal knots, the results of which will be presented in a future paper. Our result suggests that the frequency of kpc-scale triples in optically selected AGNs at $z \sim 0.1$ is $f_{\text{kpc, triple}} \gtrsim 3 \times 10^{-3} \times \frac{7}{92} \times \frac{1}{5} \approx 5 \times 10^{-5}$. If we assume that AGNs in successive mergers are independent events with short duty cycles, the expected frequency of kpc-scale triple AGNs based on the observed frequency of doubles would be $\sim f_{\text{kpc, double}}^2 \gtrsim 10^{-5}$. Our observed frequency of triples implies a higher probability than this, which may suggest that AGNs in mergers are somewhat correlated, although better statistics is needed to draw any firm conclusion.

While our slit spectra of the three nuclei suggest that they all host AGNs, optical identification alone is inconclusive. Alternatively, there could be only two or even just one active SMBH, ionizing all the three gas components in the merging system. To discriminate between these scenarios, arguments based on the ionization parameter and effective size of the narrow-line region are not very useful (e.g., Liu et al. 2010; Shen et al. 2011), because the separation between the nuclei are not much larger than the individual size of the gas-emitting regions, and the electron density measurements are highly uncertain (Table 2). *Chandra* X-ray observations could help pin down the triple AGN nature of the system.

We thank an anonymous referee for a prompt and helpful report. Support for the work of X.L. was provided by NASA through Einstein Postdoctoral Fellowship grant number PFO-110076 awarded by the Chandra X-ray Center, which is operated by the Smithsonian Astrophysical Observatory for NASA under contract NAS8-03060. Y.S. acknowledges support from a Clay Postdoctoral Fellowship through the Smithsonian Astrophysical Observatory. M.A.S. acknowledges the support of NSF grant AST-0707266.

Funding for the SDSS and SDSS-II has been provided by the Alfred P. Sloan Foundation, the Participating Institutions, the National Science Foundation, the U.S. Department of Energy, the National Aeronautics and Space Administration, the Japanese Monbukagakusho, the Max Planck Society, and the Higher Education Funding Council for England. The SDSS Web site is <http://www.sdss.org/>.

The SDSS is managed by the Astrophysical Research Consortium for the Participating Institutions. The Participating Institutions are the American Museum of Natural History, Astrophysical Institute Potsdam, University of Basel, University of Cambridge, Case Western Reserve University, University of Chicago, Drexel University, Fermilab, the Institute for Advanced Study, the Japan Participation Group, Johns Hopkins University, the Joint Institute for Nuclear Astrophysics, the Kavli Institute for Particle Astrophysics and Cosmology, the Korean Scientist Group, the Chinese Academy

of Sciences (LAMOST), Los Alamos National Laboratory, the Max-Planck-Institute for Astronomy (MPIA), the Max-Planck-Institute for Astrophysics (MPA), New Mexico State University, Ohio State University, University of Pittsburgh,

University of Portsmouth, Princeton University, the United States Naval Observatory, and the University of Washington.
Facilities: Sloan, ARC (DIS)

REFERENCES

- Abazajian, K. N., et al. 2009, *ApJS*, 182, 543
Amaro-Seoane, P., Sesana, A., Hoffman, L., Benacquista, M., Eichhorn, C., Makino, J., & Spurzem, R. 2010, *MNRAS*, 402, 2308
Amram, P., Mendes de Oliveira, C., Plana, H., Balkowski, C., & Hernandez, O. 2007, *A&A*, 471, 753
Baldry, I. K., Glazebrook, K., Brinkmann, J., Ivezić, Ž., Lupton, R. H., Nichol, R. C., & Szalay, A. S. 2004, *ApJ*, 600, 681
Baldwin, J. A., Phillips, M. M., & Terlevich, R. 1981, *PASP*, 93, 5
Barth, A. J., Bentz, M. C., Greene, J. E., & Ho, L. C. 2008, *ApJ*, 683, L119
Becker, R. H., White, R. L., & Helfand, D. J. 1995, *ApJ*, 450, 559
Begelman, M. C., Blandford, R. D., & Rees, M. J. 1980, *Nature*, 287, 307
Bernardi, M., et al. 2003, *AJ*, 125, 1866
Binney, J., & Tremaine, S. 1987, *Galactic dynamics*, ed. Binney, J. & Tremaine, S.
Blaes, O., Lee, M. H., & Socrates, A. 2002, *ApJ*, 578, 775
Bruzual, G., & Charlot, S. 2003, *MNRAS*, 344, 1000
Cardelli, J. A., Clayton, G. C., & Mathis, J. S. 1989, *ApJ*, 345, 245
Djorgovski, S. G., Courbin, F., Meylan, G., Sluse, D., Thompson, D., Mahabal, A., & Glikman, E. 2007, *ApJ*, 662, L1
Dubinski, J., Mihos, J. C., & Hernquist, L. 1999, *ApJ*, 526, 607
Greene, J. E., & Ho, L. C. 2006, *ApJ*, 641, 117
Heckman, T. M., Ptak, A., Hornschemeier, A., & Kauffmann, G. 2005, *ApJ*, 634, 161
Helou, G., Khan, I. R., Malek, L., & Boehmer, L. 1988, *ApJS*, 68, 151
Hernquist, L. 1989, *Nature*, 340, 687
Ho, L. C. 2008, *ARA&A*, 46, 475
Ho, L. C., Filippenko, A. V., & Sargent, W. L. W. 1997, *ApJS*, 112, 315
Ho, L. C., Greene, J. E., Filippenko, A. V., & Sargent, W. L. W. 2009, *ApJS*, 183, 1
Hoffman, L., & Loeb, A. 2007, *MNRAS*, 377, 957
Iwasawa, M., Funato, Y., & Makino, J. 2006, *ApJ*, 651, 1059
Kauffmann, G., et al. 2003, *MNRAS*, 346, 1055
Kewley, L. J., Groves, B., Kauffmann, G., & Heckman, T. 2006, *MNRAS*, 372, 961
Kormendy, J., & Richstone, D. 1995, *ARA&A*, 33, 581
Liu, X., Greene, J. E., Shen, Y., & Strauss, M. A. 2010, *ApJ*, 715, L30
Liu, X., Shen, Y., & Strauss, M. A. 2011a, arXiv:1104.0951
Liu, X., Shen, Y., Strauss, M. A., & Hao, L. 2011b, arXiv:1104.0950
Liu, X., Zakamska, N. L., Greene, J. E., Strauss, M. A., Krolik, J. H., & Heckman, T. M. 2009, *ApJ*, 702, 1098
Lousto, C. O., & Zlochower, Y. 2008, *Phys. Rev. D*, 77, 024034
Lutz, D., Veilleux, S., & Genzel, R. 1999, *ApJ*, 517, L13
Merritt, D. 2006, *Reports on Progress in Physics*, 69, 2513
Milosavljević, M., & Merritt, D. 2001, *ApJ*, 563, 34
Moshir, M., Kopman, G., & Conrow, T. A. O. 1992, *IRAS Faint Source Survey*, Explanatory supplement version 2, ed. Moshir, M., Kopman, G., & Conrow, T. A. O.
Osterbrock, D. E. 1989, *Astrophysics of gaseous nebulae and active galactic nuclei*, ed. Osterbrock, D. E.
Panessa, F., Bassani, L., Cappi, M., Dadina, M., Barcons, X., Carrera, F. J., Ho, L. C., & Iwasawa, K. 2006, *A&A*, 455, 173
Peng, C. Y., Ho, L. C., Impey, C. D., & Rix, H. 2010, *AJ*, 139, 2097
Renaud, F., Appleton, P. N., & Xu, C. K. 2010, *ApJ*, 724, 80
Shen, Y., Liu, X., Greene, J. E., & Strauss, M. A. 2011, *ApJ*, 735, 48
Skrutskie, M. F., et al. 2006, *AJ*, 131, 1163
Tody, D. 1986, in *Society of Photo-Optical Instrumentation Engineers (SPIE) Conference Series*, ed. D. L. Crawford, Vol. 627, 733
Toomre, A., & Toomre, J. 1972, *ApJ*, 178, 623
Tremaine, S., et al. 2002, *ApJ*, 574, 740
Valtonen, M. J. 1996, *MNRAS*, 278, 186
Veilleux, S., & Osterbrock, D. E. 1987, *ApJS*, 63, 295
Voges, W., et al. 1999, *A&A*, 349, 389
York, D. G., et al. 2000, *AJ*, 120, 1579
Yu, Q. 2002, *MNRAS*, 331, 935